Preparation and dispersion of Ni–Cu composite nanoparticles

Yu-Guo Guo,† Li-Jun Wan,* Jian-Ru Gong and Chun-Li Bai*

*Institute of Chemistry, Chinese Academy of Sciences, Beijing 100080, P.R. China.
E-mail: lijun_wan@yahoo.com; Fax: +86-10-62558934*

Finely dispersed sandwich composite nanoparticles of Cu–Ni–Cu were prepared by a novel method combining template synthesis and an ultrasonic treatment method. The composite nanoparticles have uniform cylinder shape with tunable diameter and length. Transmission electron microscopy (TEM) and electron diffraction (ED) were employed to characterize the nanoparticles. This method can be used to fabricate shape- and size-controlled composite nanoparticles in a wide range of metals and other materials. The so-prepared particles may be suitable candidates as nanoscale blocks for assembling nanodevices.

1. Introduction

In the past decade, metal and semiconductor nanoparticles have attracted much attention because of their novel optical, catalytic, electrical and magnetic properties, and their applications in building advanced materials as nanoscale building blocks.[1–3] For these purposes, size- and shape-controlled composite nanoparticles with well-defined structure may be favored. Nowadays, many methods, including ball milling,[4] pulsed electrodeposition,[5] thermal plasma,[6] polyol process,[7] gas deposition,[8] γ-radiation[9] and hydrothermal-reduction,[10] have been developed for preparation of nanosized metal particles. Recently, Peng[11] and Puntes[12] reported the size- and shape-controlled preparations of CdSe and Co nanocrystals by the injection of an organometallic precursor into a hot surfactant mixture under inert atmosphere. However, it is still a challenge to prepare size- and shape-controlled composite nanoparticles with special properties and high efficiency. Here we report a novel method to produce highly crystalline sandwich Cu–Ni–Cu composite nanoparticles.

2. Experimental

Fabrication of the sandwich cylinder-shaped Cu–Ni–Cu nanoparticles was carried out by using the process shown schematically in Fig. 1. The porous anodic aluminum oxide (AAO) templates were grown by potentiostatically anodizing aluminum plates (0.2 mm in thickness, 99.999% in purity) in aqueous solutions of 14% H_2SO_4 for obtaining pore sizes of 30 nm. After the anodization, the remaining aluminum was etched in a 20% HCl–0.1 mol L^{-1} $CuCl_2$ mixed solution. Then, the barrier layer was dissolved in 5% H_3PO_4. Finally, a silver film was deposited by vacuum evaporation onto a surface of the template membrane to provide a conductive contact. The order of the pore array, the pore density and the external shape of AAO templates were characterized by AFM topography examinations with a CSPM-2000We atomic force microscope (Ben Yuan Ltd., China). Ultralever® Si_3N_4 conical tips were used. All of the AFM images were acquired in a contact mode.

Ni/Cu composite nanowires were prepared in a single sulfate bath by using potentiostatic control and a pulsed deposition technique similar to that used for thin film deposition.[13]

† Also at Graduate School of CAS, Beijing, China.

The AAO template with Ag substrate was used as working electrode in a glass cell with a platinum counter electrode and a saturated calomel electrode (SCE) reference electrode. All electrode potentials here are reported with respect to the SCE. The nobler element Cu was kept in so dilute a concentra-
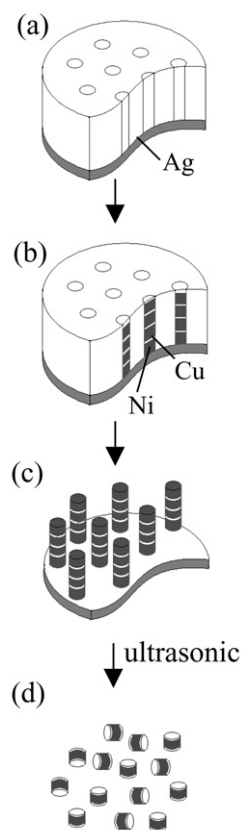

Fig. 1 Schematic illustration for fabricating Cu–Ni–Cu composite nanoparticles: (a) porous alumina with Ag backing; (b) electrodeposition of Ni–Cu multistripe nanowires; (c) removal of AAO template; (d) sandwich-like composite nanoparticles of Cu–Ni–Cu.

DOI: 10.1039/b201332k

tion that the rate of reduction of Cu was diffusion limited. The concentration of Cu ions was 1% of the concentration of Ni ions. The plating potential was alternately pulsed between -0.3 V corresponding to the reduction potential of copper, and -1.40 V to the reduction potential of nickel. A single electrolyte bath containing nickel sulfate (2 mol L^{-1}), copper sulfate (0.02 mol L^{-1}) and boric acid (0.5 mol L^{-1}) was employed at room temperature (25 °C).[13] The pH of the electrolyte solution was controlled between $3.5-4.0$. The removal of Ni–Cu nanowires from AAO matrix was done by dissolving the AAO template in 2 mol L^{-1} NaOH at 25 °C for 80 min.

The dispersion of Cu–Ni–Cu nanoparticles was carried out with a Bransonic Ultrasonic Cleaner (B-2200 E4) with working frequency ~47 kHz and power supply 205 W. The TEM experiment was carried out with a Philips TECNAI-20 operated at 120 kV for the study of the morphology and microstructure of Ni–Cu nanowires and Ni–Cu composite nanoparticles.

3. Results and discussion

Nano-scale templates play an important role in forming nanowires and in fabricating composite nanoparticles. The quality and distribution of the pore size of the AAO template was examined by AFM. Fig. 2 is a typical AFM image of the AAO template used in our experiment. From the image, a honeycomb structure, characterized by a close-packed array of columnar hexagonal cells can be seen. Each cell contains a central pore normal to the surface. The average diameter of the pore was about 30 nm with a density of 1.2×10^{10} pores cm^{-2}. This indicates that a relatively simple process compared with the two-step anodizing process can prepare AAO template with well-defined structure.[14]

Fig. 3a and b are TEM images of Ni–Cu–Ni and Cu–Ni–Cu multistripe nanowires respectively. Fig. 3a shows a bundle of Ni–Cu–Ni nanowires. Fig. 3b shows well-dispersed Cu–Ni–Cu nanowires. The diameter of a wire is about 30 nm consistent with the diameter of the apertures of the AAO template. Ni segments and Cu segments can be clearly seen in the images of their different configurations. The Ni segments are continuous in the smooth surface, while the Cu segments are made up of several particles in the rough surface.

Fig. 4 is a high-magnification TEM image obtained in Ni–Cu multistripe nanowires. The feature of Ni stripes alternated
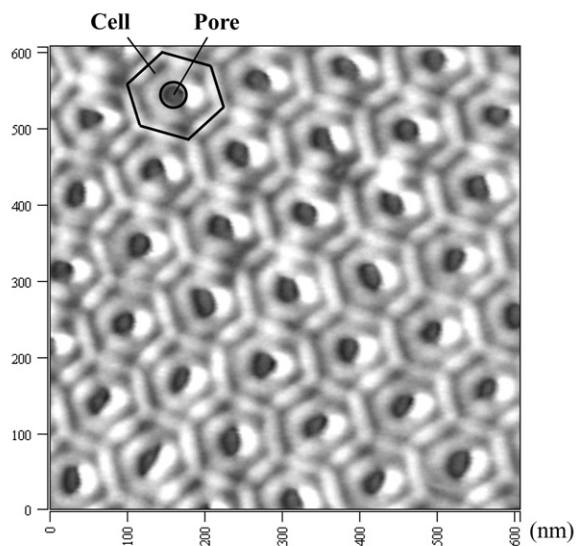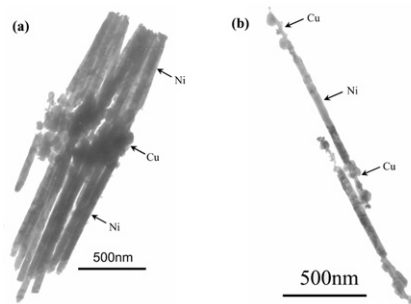

Fig. 3 TEM images of (a) a bundle of Ni–Cu–Ni composite nanowires, and (b) dispersed Cu–Ni–Cu composite nanowires.

with Cu stripes is clearly seen in the image. The physical basis of the electron contrast in the TEM image is the crystallization and the difference in atomic weights, which results in the electron dispersing ability of Ni segments being stronger than that of Cu segments, and hence the darker sections correspond to Ni and the brighter sections correspond to Cu. The nanowires were electrodeposited at -1.4 V for 10 s of Ni segments and -0.30 V for 30 s of Cu segments in the porous AAO template with pore diameters of 30 nm. From the image of Fig. 4, Ni–Cu composite nanowires with almost the same length (7 nm) Cu segments and various length Ni segments (30, 32, 34, 34, 34 and 34 nm) (bottom to top) can be seen. The lengths of Cu and Ni segments are controllable by varying deposition time. Note that small globules can be seen around the nanowire shown in Fig. 3. These globules may be Cu particles produced during ultrasonic treatment. Although the composite nanowire was prepared epitaxially by electrodeposition, the Cu section with short length should be weaker than the Ni section. On the other hand, the Cu section may be not well crystallized in the deposition process and consist of copper particles. This is also the reason that different contrast can be seen in the TEM image although there is a small difference in the atomic weight of Cu and Ni. Under ultrasonic treatment, the fracture of the nanowire will start in the Cu section and small particles are produced. The particles will adsorb on the Cu section of nanowire. However, if the nanowire was cleared, a uniform nanowire like those in Fig. 4 can be seen.

TEM images in Fig. 5 show the sandwich cylinder-shaped Cu–Ni–Cu composite nanoparticles. These images show well-defined sandwich cylinder-shaped Cu–Ni–Cu composite nanoparticles with an average diameter of 31 nm and an average length of 33 nm. The ED pattern in Fig. 5b shows a cubic structure with $a = 3.5225$ Å consistent to Ni crystal. It was found that a preferred growth direction of Ni nanoparticles exists. The preferred growth direction was determined as $\langle 111 \rangle$ from a comparison of the electron diffraction patterns and the corresponding images. The $\langle 111 \rangle$ direction is parallel to the cylinder axis of nanoparticles.
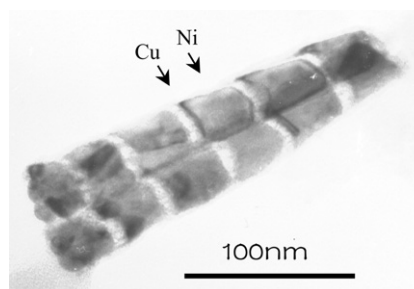

Fig. 2 AFM image of porous alumina membranes.

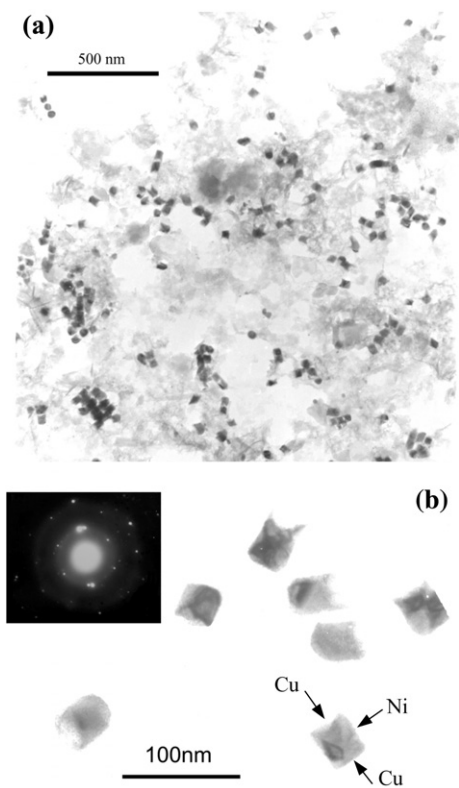**Fig. 4** High-magnification TEM image of Ni–Cu alternative composite nanowires.

Fig. 5 Low-magnification (a) and high-magnification (b) TEM images of Cu–Ni–Cu composite nanoparticles. The inset is the electron diffraction pattern of the nanoparticles. They were fabricated by ultrasonic treatment for 15 min.

Fig. 6 Typical distribution of the diameter (a) and the length (b) of the well-dispersed Cu–Ni–Cu composite nanoparticles.

Fig. 6 shows the typical distribution of the Cu–Ni–Cu composite nanoparticle size from TEM observation. The average diameter of the nanoparticles is measured to be approximately 31.2 nm and the distribution of the diameter was consistent with that of the apertures of the AAO template used. Their length may vary from ten to hundreds of nanometers controlled by the deposition time, speed, *etc*. Fig. 6b shows the typical distribution of the length of the Cu–Ni–Cu composite nanoparticles obtained at −1.4 V for 10 s. The mean length was 32.9 nm and the distribution was very narrow.

4. Conclusions

By combining the technique of template synthesis and an ultrasonic treatment method we prepared size- and length-controlled and well dispersed composite Cu–Ni–Cu nanoparticles. Ni–Cu alternative nanowires can be clearly seen in TEM images. They can be dispersed by ultrasonic treatment to obtain Cu–Ni–Cu composite nanoparticles. These cylinder-shaped nanoparticles have a preferred growth direction ⟨111⟩ parallel to each cylinder axis. If an AAO template with a square and triangular nanohole array is used, this method can be used to fabricate shape- (cylinder, cuboid, prism, *etc*.) and size-controlled composite nanoparticles in a wide range of metals and other materials. Assembling nanodevices with these composite nanoparticles will be explored in future work.
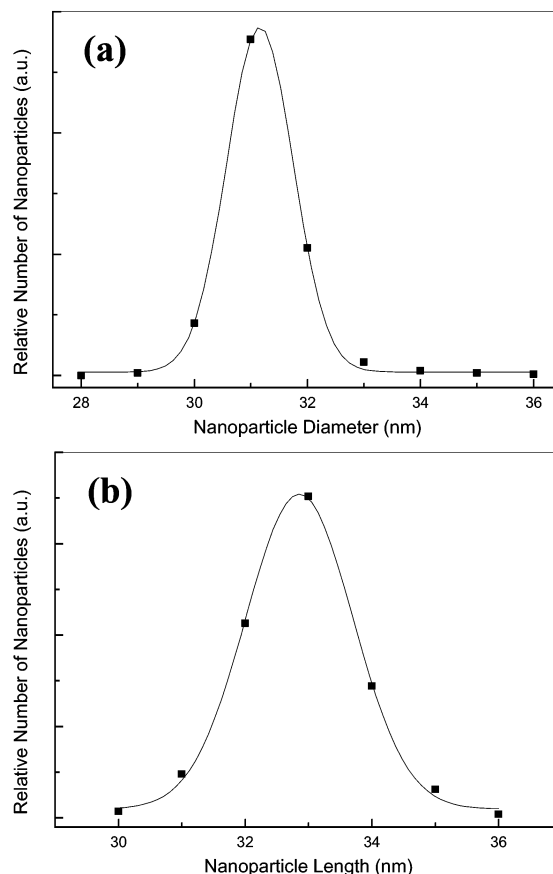
References

1 A. P. Alivisatos, *Science*, 1996, **271**, 933.
2 S. H. Sun, C. B. Murray, D. Weller, L. Folks and A. Moser, *Science*, 2000, **287**, 1989.
3 C. M. Lieber, *Solid State Commun.*, 1998, **107**, 607.
4 C. Dolitis and W. L. Johnson, *J. Appl. Phys.*, 1986, **60**, 1147.
5 H. Natter and R. Hempelmann, *J. Phys. Chem.*, 1996, **100**, 19 525.
6 Y. Morrysohi, M. Futaki, S. Komatsu and T. Ishigaki, *J. Mater. Sci. Lett.*, 1997, **16**, 347.
7 S. Puvvada, S. Bural, G. M. Chow, S. B. Qudri and B. R. Ratna, *J. Am. Chem. Soc.*, 1994, **116**, 2135.
8 M. Ichiki, J. Akedo, K. Mori and Y. Ishikawa, *J. Mater. Sci. Lett.*, 1997, **16**, 531.
9 Y. J. Zhu, Y. T. Qian, M. W. Zhang and Z. Y. Chen, *J. Mater. Sci. Lett.*, 1994, **13**, 1243.
10 C. Wang, X. M. Zhang, X. F. Qian, Y. Xie, W. Z. Wang and Y. T. Qian, *Mater. Res. Bull.*, 1998, **33**, 1747.
11 X. G. Peng, L. Manna, W. D. Yang, J. Wickham, E. Scher, A. Kadavanich and A. P. Alivisatos, *Nature*, 2000, **404**, 59.
12 V. F. Puntes, K. M. Krishnan and A. P. Alivisatos, *Science*, 2001, **291**, 2115.
13 L. Wang, K. Yu-Zhang, A. Metrot, P. Bonhomme and M. Troyon, *Thin Solid Films*, 1996, **288**, 86.
14 H. Masuda and K. Fukuda, *Science*, 1995, **268**, 1466.